Title:

Rapid degradation of methylene blue in a novel heterogeneous Fe_3O_4@rGO@TiO_2-catalyzed photo-Fenton system

---

Author names

Xiaoling Yang, Wei Chen, Jianfei Huang, Ying Zhou, Yihua Zhu,* and Chunzhong Li

Affiliations

East China University of Science and Technology, Key Laboratory for Ultrafine Materials of Ministry of Education, School of Materials Science and Engineering, Shanghai 200237, China

* Authors to whom correspondence should be addressed

yhzhu@ecust.edu.cn

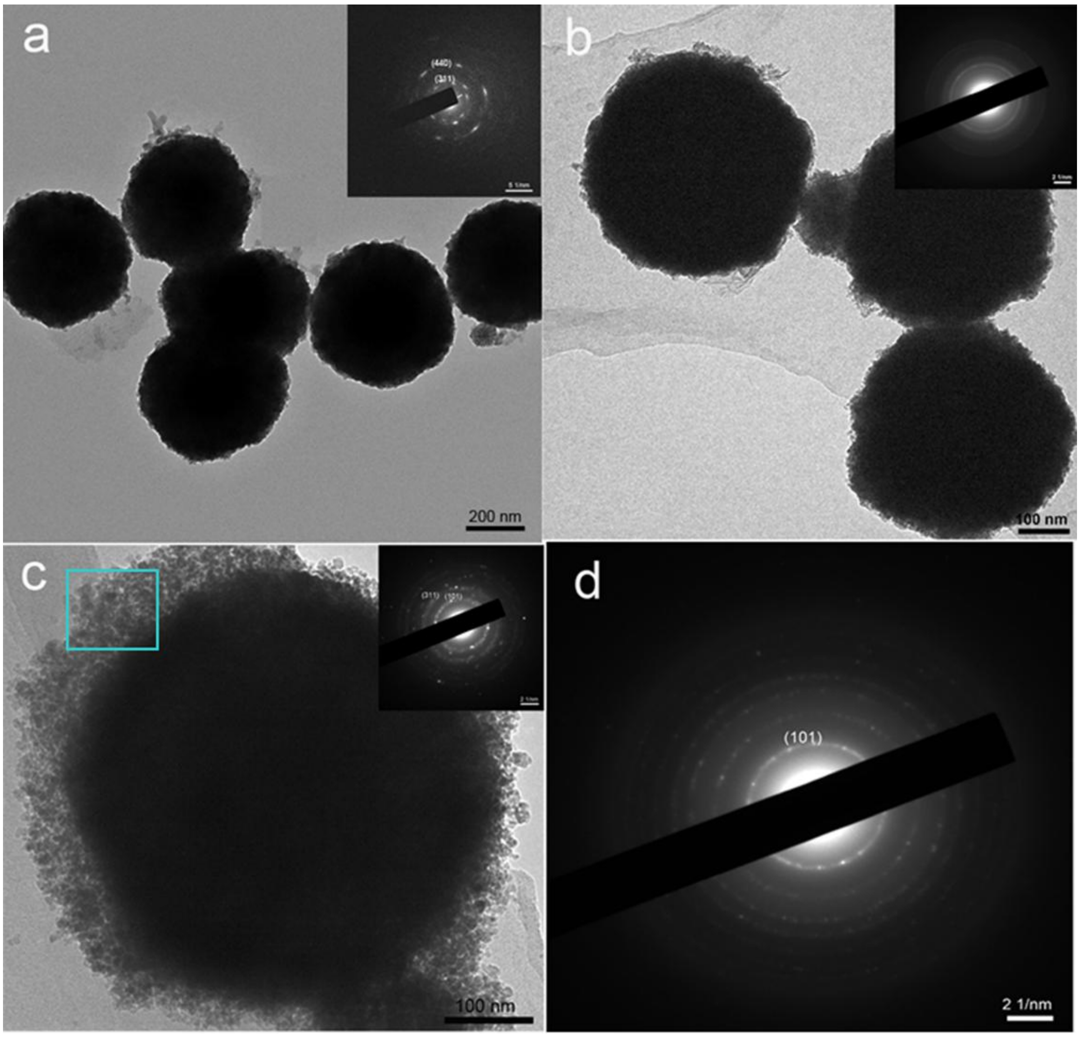

Fig. S1 (a-c) HRTEM and selected area electron diffraction (SAED) patterns of Fe_3O_4, Fe_3O_4@GO and Fe_3O_4@rGO@TiO_2; (d) SAED image of the selected area in Fig. S1c.

The SAED image of Fe_3O_4 particles shown as an inset of Fig. S1a illustrates that Fe_3O_4 is a polycrystallinity. The calculated lattice spacings from the diffraction patterns, with the values of 0.246 and 0.143 nm, match perfectly with that of (311) and (440) planes of Fe_3O_4 (JCPDS file No. 19-0629). The SAED pattern of Fe_3O_4@GO (Figure. S1b) shows only diffraction rings without any diffraction dots, which may be attributed to the existence of the amorphous GO [1,2]. Moreover, the HRTEM and SAED graph of Fe_3O_4@rGO@TiO_2 composites illustrated in Fig. S1c revealed that TiO_2 nanospheres were successfully deposited on the surface of the GO-wrapped Fe_3O_4 particles. Another electron diffraction image of the selected area in Figure. S1c with distinct diffraction rings was depicted in Figure. S1d. The lattice spacing calculated from the diffraction rings agrees well with that of (101) planes of TiO_2 (JCPDS file No. 21-1272), indicating that anatase TiO_2 was grown in Fe_3O_4@rGO@TiO_2 successfully and TiO_2 existed in the composites is also a polycrystallinity.

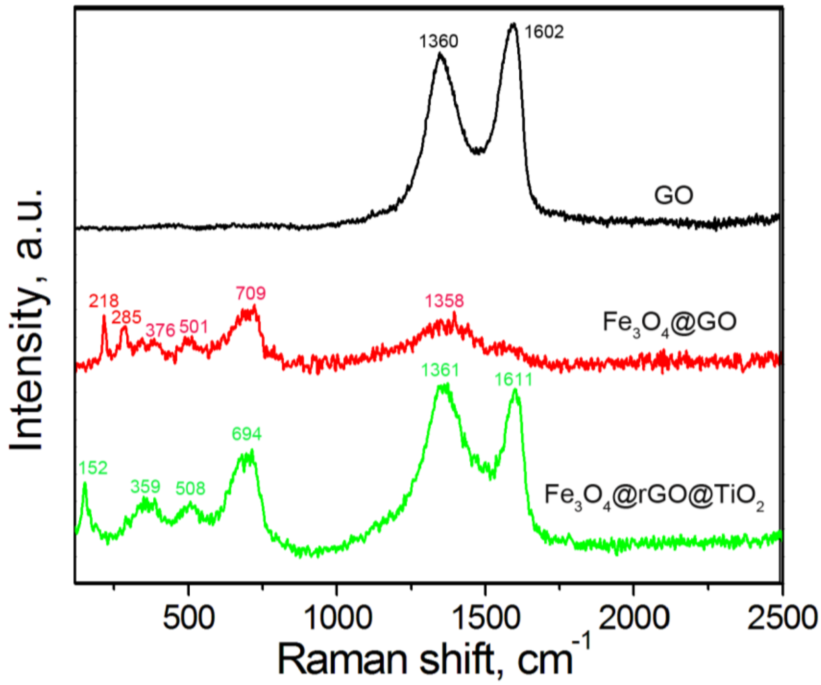

Fig. S2 Raman spectra of GO, Fe_3O_4@GO, Fe_3O_4@rGO@TiO_2.

Fig. S2 shows the Raman spectrogram of GO, Fe_3O_4@GO and Fe_3O_4@rGO@TiO_2. As can be seen in the above graph, GO shows an obvious Raman shift at 1360 and 1602 cm^{-1} corresponding to the D- and G- bands, respectively [3]. The Raman signals located at 218, 285, 376, 501 and 709 cm^{-1}, corresponding to the vibration modes of Fe-O bonds of Fe_3O_4 nanoparticles could be observed in

Fe_3O_4@GO [4]. The reason that the D- and G- bands of GO centered at 1358 cm^{-1} in Fe_3O_4@GO may be due to overlap of two peaks, one of Fe_3O_4 at 1300 cm^{-1} [5] and a GO D band peak at 1360 cm^{-1}. Some new peaks occurred at 152, 359, 508, 694 cm^{-1} when TiO_2 nanoparticles were decorated on the surface of the GO-wrapped Fe_3O_4, all of which are characteristic peaks of anatase TiO_2 [6]. Besides, the intensity ratio of D- and G- bands of GO (I_D/I_G) changed after depositing TiO_2 nanoparticles on the surface of the GO-encapsulated Fe_3O_4 nanospheres through the hydrothermal reaction, indicating that the structure defects increased after GO was transformed into rGO partially. The raman spectrum of Fe_3O_4@rGO@TiO_2 is actually a simple combination of that of Fe_3O_4, rGO and TiO_2. This illustrates that the combination of the three components is just a physical force.

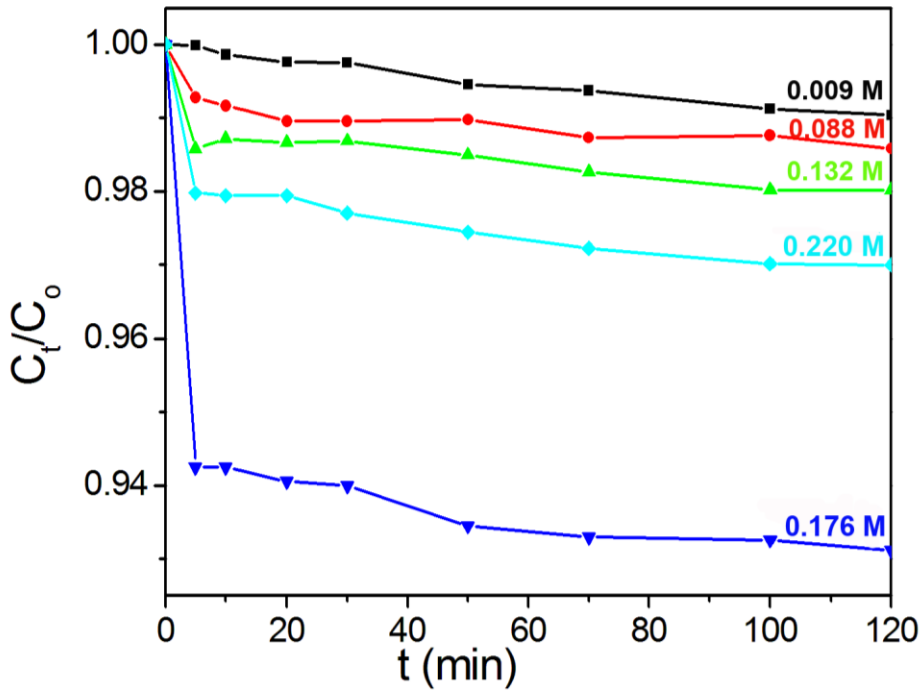

Fig. S3 Effect of dose of H_2O_2 on the degradation of MB without any catalysts at room temperature and neutral pH.

As can be seen in the Fig. S3, different dose of H_2O_2 just have slight effect on the degradation of MB and the degradation tendency is similar to the consequence shown in Fig 4b. These results further confirm that the as-prepared catalysts do have a great effect on the degradation of MB, and the degradation efficiency can increase as the amount of H_2O_2 increasing until an optimal point, and a slight decreasing will occur when the amount of H_2O_2 is beyond the optimum which can be attributed to the side reaction between H_2O_2 and ·OH.

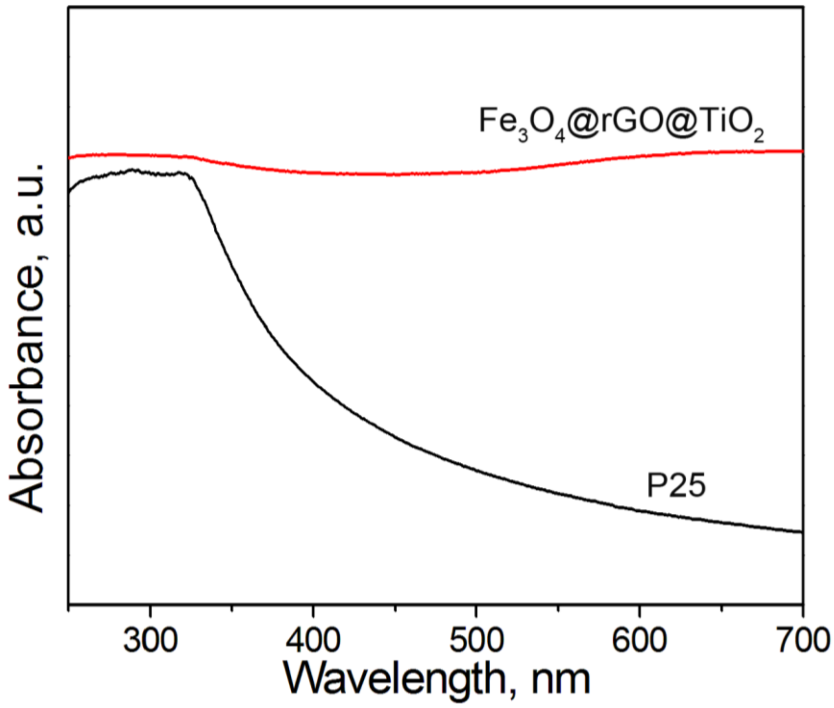

Fig. S4 UV-visible spectra of P25 and Fe_3O_4@rGO@TiO_2

It can be observed from Fig. S4 that Fe_3O_4@rGO@TiO_2 has a more intensive absorption of visible light compared with P25 due to coexistence of rGO and Fe_3O_4. Besides, a red shift in the absorption edge is clearly presented, illustrating that the band gap of TiO_2 has been narrowed and the electrons in the valance band can be excited to the conduction band under the visible illumination.

[1] Xie, G. Q. *et al.* A facile chemical method to produce superparamagnetic graphene oxide-Fe_3O_4 hybrid composite and its application in the removal of dyes from aqueous solution. *J. Mater. Chem.* **22,** 1033-1039 (2012).

[2] Wang, G. X. *et al.* Facile synthesis and characterization of graphene nanosheets. *J. Phys. Chem. C* **112,** 8192-8195 (2008).

[3] Sher Shah, M. S. A., Park, A. R., Zhang, K., Park, J. H., Yoo, P. J. Green synthesis of biphasic TiO_2-reduced graphene oxide nanocomposites with highly enhanced photocatalytic activity. *ACS Appl. Mater. Interfaces* **4,** 3893-3901 (2012).

[4] Hu, X. B. *et al.* Adsorption and heterogeneous Fenton degradation of 17α-methyltestosterone on nano Fe_3O_4/MWCNTs in aqueous solution. *Appl. Catal., B* **107,** 274-283 (2011).

[5] Wang, J. Z. *et al.* Graphene - encapsulated Fe_3O_4 nanoparticles with 3D laminated structure as superior anode in lithium ion batteries. *Chem. Eur. J.* **17,** 661-667 (2011).

[6] Jang, B. J. *et al.* In situ growth of TiO_2 in interlayers of expanded graphite for the fabrication of TiO_2-graphene with enhanced photocatalytic activity. *Chem. Eur. J.* **17,** 8379-8387 (2011).